Int. J. Heat Mass Transfer. Vol. 22, pp. 1095–1105
© Pergamon Press Ltd. 1979. Printed in Great Britain

0017-9310/79/0701-1095 $02.00/0

EFFECTS OF RADIATION AND CONVECTIVE BOUNDARY CONDITIONS ON THE STABILITY OF FLUID IN AN INCLINED SLENDER SLOT

M. A. HASSAB† and M. N. ÖZIŞIK
Department of Mechanical and Aerospace Engineering,
North Carolina State University, Raleigh, North Carolina 27650, U.S.A.

(*Received* 7 *July* 1978 *and in revised form* 27 *November* 1978)

Abstract—The neutral stability of an absorbing, emitting, scattering, nongray viscous fluid contained inside an inclined slender slot and subjected to convective boundary conditions is examined for inclination from 0° to 180°. The modified P-1 approximation (Eddington approximation) is employed for the radiation part of the problem. The effects of the Biot numbers H_1 and H_2 at the lower and upper surfaces, the conduction-to-radiation parameter, N, optical thickness τ_0, single scattering albedo ω, the wall emissivities ε_1 and ε_2, the nongrayness factor η and the inclination angle δ on the onset of stability in gases are determined for both the longitudinal and transverse vortex rolls. The results show that radiation besides its stabilizing effect significantly shifts the transition angle for cross over from the transverse to the longitudinal rolls towards horizontal.

NOMENCLATURE

a, magnitude of the wave vector, $a = \sqrt{a_1^2 + a_2^2}$;
a_1, wave number in x-direction;
a_2, wave number in z-direction;
c, a complex number;
c_p, constant-pressure specific heat of fluid;
d, width of the slot;
D, operator, $\frac{\mathrm{d}}{\mathrm{d}y}$;
g, acceleration of gravity;
Gr^*, external Grashof number, $\gamma g(T_{\infty 1} - T_{\infty 2})d^3/\nu^2$;
Gr, internal Grashof number, $\gamma g(\bar{T}_{w1} - \bar{T}_{w2})d^3/\nu^2$;
h_1, heat transfer coefficient at the lower surface;
h_2, heat transfer coefficient at the upper surface;
H_1 Biot number at the lower surface, $H_1 = h_1 d/k$;
H_2, Biot number at the upper surface, $H_2 = h_2 d/k$;
j', perturbed incident radiation;
$\hat{j}$, dimensionless perturbed incident radiation, $j'/4\bar{\sigma}\bar{T}_0^3(T_{\infty 1} - T_{\infty 2})$;
k, thermal conductivity of the fluid;
L, height of the slot;
N, conduction-to-radiation parameter, $\frac{k\bar{\beta}}{4\bar{\sigma}\bar{T}_0^3}$;
p', perturbed pressure;
$\hat{p}$, dimensionless perturbed pressure, $p'/\left(\frac{\mu u_0}{d}\right)$;
Pr, Prandtl number, ν/α;
$\bar{q}_r$, dimensionless initial radiative heat-flux, $\bar{Q}_r/4\bar{\sigma}\bar{T}_0^3(T_{\infty 1} - T_{\infty 2})$;
$R\bar{a}^*$, external Reyleigh number, $G\bar{r}^* \cdot Pr$;
Ra, internal Rayleigh number, $Gr \cdot Pr$;
t, time;
T', perturbed fluid temperature;
$\bar{T}_0$, constant mean temperature;
$T_{\infty 1}$, $T_{\infty 2}$, environment temperatures at the lower and upper surfaces, respectively;
$\bar{T}_{w1}$, $\bar{T}_{w2}$, mean temperatures of lower and upper walls, respectively for the initial (i.e., base flow) situation;
u', v', w', perturbed velocity components;
$\hat{u}, \hat{v}, \hat{w}$, dimensionless perturbed velocity components $(u', v', w')/u_0$;
u_0, characteristic velocity, $\gamma g(T_{\infty 1} - T_{\infty 2})d^2/\nu$;
$\bar{u}_v$, dimensionless base flow velocity at vertical position, $\bar{U}_v/u_0$;
X, Y, Z, Cartesian coordinates with Y measured normal to the fluid layer;
x, y, z, $(X, Y, Z)/d$.

Greek symbols

α, thermal diffusivity;
$\bar{\beta}$, mean extinction coefficient, $\bar{\beta} = \sqrt{(\sigma + \kappa_p)(\sigma + \kappa_R)}$;
γ, coefficient of thermal expansion for fluid;
Γ, $= \left|\omega + \frac{1-\omega}{\eta^2}\right|^{-1/2}$;
δ, angle measured from horizontal;
ε_1, ε_2, emissivities of lower and upper surfaces, respectively;
η, nongrayness factor, $(\kappa_p/\kappa_R)^{1/2}$;
$\hat{\theta}$, dimensionless perturbed temperature, $T'/(T_{\infty 1} - T_{\infty 2})$;

†Presently, Mechanical Engineering Department, Valparaiso University, Valparaiso, IN 46383, U.S.A.

κ_p, κ_R, Planck mean and Rosseland mean coefficients, respectively;
λ_i, $= \frac{3}{2}\varepsilon_i\tau_0/(2-\varepsilon_i)\Gamma$; $i = 1,2$;
ν, kinematic viscosity;
ψ, dimensionless stream function;
ξ_i, $= 2(2-\xi_i)\tau_0(1-\omega)\Gamma/\xi_i$; $i = 1,2$;
ρ, density of fluid;
σ, scattering coefficient for fluid;
$\bar{\sigma}$, Stefan–Boltzmann constant;
τ, dimensionless time, $\tau = \nu t/d^2$;
τ_0, optical thickness of the fluid, $\tau_0 = \bar{\beta}\cdot d$;
ω, single scattering albedo, $\omega = \sigma/(\sigma+\kappa_p)$;
∇^2, $= \left(\frac{\partial^2}{\partial x^2}+\frac{\partial^2}{\partial y^2}+\frac{\partial^2}{\partial z^2}\right)$;
Λ, $= \frac{d^2}{\nu U_0^2}\left[\frac{1}{\rho_0}\frac{dP}{dX}-g\right]$.

Superscripts

$-$, mean quantities;
$'$, $\hat{}$, $*$, $^+$, refer to perturbed quantities.

Subscripts

∞, refers to outside environment;
0, fixed quantities.

INTRODUCTION

THE EFFECT of radiation on the initiation of the convective motion in fluids confined between two horizontal isothermal plates with lower plate hotter than the upper one (i.e., Bénard Problem) has been of interest during the last three decades. The earlier studies of such stability problems were restricted to gray fluids [1–3] and the radiation part of the problem was treated approximately by using the optically thin or the optically thick limit approximation. Spiegel [4] considered the Bénard type problem for a gray fluid for the entire range of the optical thickness, but neglected the effect of conduction and the radiation boundary conditions from the perturbed integral form of the equation of radiative transfer. An experimental and theoretical investigation of the effects of radiation on the onset of convection in dry air and ammonia contained between two isothermal plates, has been published by Gille and Goody [5]. They considered the spectral effect of nongrayness on the onset of convection and experimentally demonstrated that radiation delayed the onset of instability. Arpaci and Gözüm [6] employed the Eddington approximation (i.e., P-1 approximation) to study the effects of radiation from the boundaries and included the nongrayness effects of gases on the stability of an absorbing, emitting fluid contained between two infinitely horizontal rigid (or free) planes at different isothermal temperatures. They checked the accuracy of the "P-1, P-3 and P-5 approximations" in a stability problem by comparing the approximate solutions with the exact solution of Spiegel [4]. Arpaci and Bayazitoğlu [7] investigated the effects of radiation on the neutral instability of natural flow of gases in a slender slot between two very long vertical plates at two different isothermal temperatures for an absorbing and emitting fluid by using the Eddington approximation, and included the nongrayness of the fluid. Their results indicate that the relative effect of radiation is much less in magnitude for the vertical case than the case of horizontal. Recently, Özişik and Hassab [8] studied the thermal instability of a radiating gas between two inclined parallel plates heated from below and subjected to convective boundary condition at the upper surface. Their analysis was restricted to inclinations such that the longitudinal disturbances were dominant.

The foregoing review of the literature reveals that thermal instability of radiating fluids in slots for inclinations from 0 to 180° has not yet been investigated. Therefore, this analysis is devoted to the study of stability of an absorbing, emitting, isotropically scattering nongray fluid contained in an inclined slot having a very large aspect ratio and subjected to convective boundary conditions at both boundaries. Also included is the stability of a horizontal layer of radiating fluid heated from below and subjected to a free surface at the upper boundary.

ANALYSIS

Consider a layer of fluid contained inside a slot inclined from the horizontal by an angle δ, as shown in Fig. 1. The slot has the dimensions L for height and d for width with the assumption that the aspect ratio $L/d \gg 1$. If a small temperature difference is imposed across the layer of the fluid in the direction normal to the sidewalls, a unicellular motion sets up in such a manner that the fluid near the hot plate rises upward and that near the cold plate descends down. If this temperature difference is gradually increased, the initial laminar motion between the plates breaks up and secondary flow appears in the form of two-dimensional multicellular convective motion. The main purpose in this study is to investigate the effect of radiation on the onset of secondary flow. In the present analysis it is assumed that the flow is incompressible, laminar, Newtonian, and has constant physical properties except for the density which appears in the body forces (i.e., Boussinesq approximation). It is assumed further that viscous dissipation and the work of compression

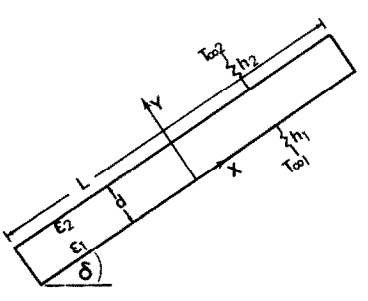

FIG. 1. Inclined slot.

are negligible. The analysis is restricted to the so-called *conduction* regime, which requires that the aspect ratio of the slot is very large [9, 10].

Governing general equations

The equations of motion and energy that are basic for the analysis of the instability of fluids can be written in the general form, using the vector notation as

$$\text{Continuity:} \qquad \nabla \cdot \mathbf{V} = 0 \tag{1}$$

Momentum:

$$\frac{D\mathbf{V}}{Dt} = -\frac{1}{\rho_0}\nabla P - (1-\gamma\cdot\Delta T)g(\hat{i}\sin\delta + \hat{j}\cos\delta) + \nu\nabla^2\mathbf{V} \tag{2}$$

$$\text{Energy:} \qquad \frac{DT}{Dt} = \alpha\nabla^2 T - \frac{\kappa_p}{\rho_0 c_p}(4\bar{\sigma}T^4 - J), \tag{3}$$

where

$$\nabla = \frac{\partial}{\partial X}\hat{i} + \frac{\partial}{\partial Y}\hat{j} + \frac{\partial}{\partial Z}\hat{k},$$

$$\mathbf{V} = U\hat{i} + V\hat{j} + W\hat{k},$$

$$\Delta T = T - T_{\infty 2},$$

with U, V and W are the velocity components in the X, Y, and Z directions respectively. J, P and T are the incident radiation, dynamic pressure and the temperature respectively; ρ_0 and c_p are the density and specific heat at constant pressure, α is the thermal diffusivity, ν is the kinematic viscosity, γ is the thermal expansion coefficient for the fluid; t is the time, δ is the angle measured from the horizontal; $\hat{i}$, $\hat{j}$ and $\hat{k}$ stand for the unit vectors in the X, Y and Z directions respectively and g is the gravity.

The incident radiation term J appearing in the above energy equation should be obtained from the solution of the equation of radiative transfer subjected to appropriate radiative boundary conditions for the problem. However, the exact solution of the equation of radiative transfer with the presence of scattering is a very complicated matter. It is for this reason we use the P-1 approximation of the spherical harmonics method by including the effects of isotropic scattering. The P-1 equation is modified to allow for the nongrayness effects of the gas by following the ideas suggested in [11–13]; the resulting equation for the scalar quantity J, is given as

$$\nabla^2 J - 3\kappa_p(\kappa_R + \sigma)J = -48\kappa_p(\kappa_R + \sigma)\bar{\sigma}T^4, \tag{4}$$

where κ_p, κ_R and σ are the Planck mean absorption, Rosseland mean absorption and mean scattering coefficients respectively and $\bar{\sigma}$ is the Stefan–Boltzmann constant.

Base flow analysis

The equations governing the initial motion of the fluid in an inclined slot having a very large aspect ratio (i.e., $L/d \gg 1$), under the modified P-1 approximation for the radiation part of the problem, are given in the dimensionless form as:

x-momentum:

$$\frac{d^2\bar{u}}{dy^2} + \bar{\theta}\sin\delta = \Lambda \tag{5a}$$

Energy:

$$\frac{d}{dy}\left[\frac{d\bar{\theta}}{dy} - \frac{\tau_0}{N}\bar{q}_r\right] = 0 \tag{6a}$$

Radiation:

$$\frac{d^2\bar{q}_r}{dy^2} - 3(1-\omega)\tau_0^2\bar{q}_r = 4(1-\omega)\tau_0\Gamma\frac{d\bar{\theta}}{dy}, \tag{7a}$$

with the following boundary conditions for $\bar{u}$ and $\bar{\theta}$:

$$\bar{u} = 0, \quad \text{at} \quad y = 0,1 \tag{5b}$$

$$\left[\frac{d\bar{\theta}}{dy} - \frac{\tau_0}{N}\bar{q}_r\right] - H_1\bar{\theta} = -H_1, \quad \text{at} \quad y = 0 \tag{6b}$$

$$\left[\frac{d\bar{\theta}}{dy} - \frac{\tau_0}{N}\bar{q}_r\right] + H_2\bar{\theta} = 0, \quad \text{at} \quad y = 1, \tag{6c}$$

and the Marshak boundary conditions for opaque walls [14]:

$$\frac{d\bar{q}_r}{dy} - \xi_1\bar{q}_r = 0, \quad \text{at} \quad y = 0 \tag{7b}$$

$$\frac{d\bar{q}_r}{dy} + \xi_2\bar{q}_r = 0, \quad \text{at} \quad y = 1. \tag{7c}$$

A gross mass balance for the closed system is given as:

$$\int_0^1 \bar{u}(y)dy = 0. \tag{5c}$$

Here, $\bar{u}$, $\bar{\theta}$ and $\bar{q}_r$ are the dimensionless base flow quantities of velocity in the x-direction, temperature and the y-component of the radiative heat flux respectively; τ_0 is the optical thickness; N is the conduction-to-radiation parameter; ω is the single scattering albedo; ε_1 and ε_2 are the emissivities of the lower and upper surfaces respectively, and H_1 and H_2 are the Biot numbers at the lower and upper surfaces respectively. The thermal resistances of the walls are neglected in equations (6b) and (6c), since the walls are assumed having a thickness very small compared to that of the fluid layer [14]. It is to be noted that the one-dimensional radiative equation for the base flow analysis is written in terms of $\bar{q}_r$ instead of $\bar{J}$, because the boundary conditions of $\bar{q}_r$ become homogeneous as apparent from equations (7b) and (7c). However, for multi-dimensional case, q_r being a vector, it is convenient to write the radiation equation for the disturbances in terms of the scalar quantity J. Also, the nonlinear term dT^4/dy^4 contained in equation (7a) is linearized since the temperature variation across the fluid layer is small.

The solution of the above coupled equations (5) to (7) is somewhat lengthy, but a straight-forward matter; the resulting expressions for $\bar{\theta}(y)$ and $\bar{u}(y)$ are determined as:

$$\bar{\theta}(y) = 1 + A_1(e^{sy}-1) + A_2(1-e^{-sy}) + A_3\left[y + \frac{1+(4\Gamma/3N)}{H_1}\right] \quad (8a)$$

$$\bar{u}(y)/\sin\delta = \bar{u}_v(y) = b_1 y(y-1) - A_1\left[\frac{e^{sy}-1}{s^2} - y\frac{e^s-1}{s^2}\right] - A_2\left[\frac{1-e^{-sy}}{s^2} - y\frac{(1-e^{-s})}{s^2}\right] - \frac{A_3}{6}y(y^2-1), \quad (8b)$$

where

$$A_1 = \frac{\tau_0}{SNF}\{l_1^*[(s-\xi_2)e^{-s} - \xi_2 x_2] + l_2^*[s+\xi_1(1+x_2)]\},$$

$$A_2 = \frac{\tau_0}{SNF}\{l_1^*[(s+\xi_2)e^{s} + \xi_2 x_1] + l_2^*[s-\xi_1(1+x_1)]\},$$

$$A_3 = \frac{-R_t}{\left(1+\frac{4\Gamma}{3N}\right)}[1 + A_1(e^s-1) + A_2(1-e^{-s})],$$

$$F = [s-\xi_1(1+x_1)][(s-\xi_2)e^{-s} - \xi_2 x_2] - [s+\xi_1(1+x_2)][\xi_2 x_1 + (s+\xi_2)e^s],$$

$$s = \left[3(1-\omega)\tau_0^2\left(1+\frac{4\Gamma}{3N}\right)\right]^{1/2},$$

$$x_2 = \frac{R_t}{1+(3N/4\Gamma)}\frac{1-e^{-s}}{s},$$

$$x_1 = \frac{R_t}{1+(3N/4\Gamma)}\frac{e^s-1}{s},$$

$$l_i^* = \frac{R_t}{1+(3N/4\Gamma)}\frac{N\xi_i}{\tau_0}, \quad i = 1 \text{ or } 2,$$

$$R_t = \left[\frac{1}{H_1} + \frac{1}{H_2} + \frac{1}{1+(4\Gamma/3N)}\right]^{-1},$$

$$b_1 = \frac{1}{2}\left[\Lambda - 1 + A_1 - A_2 - \frac{1+(4\Gamma/3N)}{H_1}A_3\right],$$

$$\Lambda = 1 + A_1\left\{1 + 12\left[\left(\frac{e^s-1}{s^2}\right)\left(\frac{1}{s}-\frac{1}{2}\right) - \frac{1}{s^2}\right]\right\} - A_2\left\{1 + 12\left[\left(\frac{1-e^{-s}}{s^2}\right)\left(\frac{1}{s}+\frac{1}{2}\right) - \frac{1}{s^2}\right]\right\} + A_3\left[\frac{1}{2} + \frac{1+(4\Gamma/3N)}{H_1}\right].$$

The stability analysis

The total and perturbed quantities are defined as:

$$U = \bar{U}(Y) + u', \quad V = v', \quad W = w', \quad P = \bar{P}(X) + p', \quad T = \bar{T}(Y) + T', \quad J = \bar{J}(Y) + j'. \quad (9)$$

Introducing the total quantities U, V, W, etc. into the system of equations (1)–(4), subtracting from each of the resulting expression the corresponding base flow equation, neglecting the nonlinear terms, the following system of linear perturbation equations is obtained in the dimensionless form as:

$$\frac{\partial \hat{u}}{\partial x} + \frac{\partial \hat{v}}{\partial y} + \frac{\partial \hat{w}}{\partial z} = 0, \quad (10)$$

$$\left(\frac{\partial}{\partial \tau} - \nabla^2\right)\hat{u} + G\bar{r}^*\bar{u}_v\frac{\partial \hat{u}}{\partial x}\sin\delta + G\bar{r}^*\frac{d\bar{u}_v}{dy}\hat{v}\sin\delta = -\frac{\partial \hat{p}}{\partial x} + \hat{\theta}\sin\delta, \quad (11a)$$

$$\left(\frac{\partial}{\partial \tau} - \nabla^2\right)\hat{v} + G\bar{r}^*\bar{u}_v\frac{\partial \hat{v}}{\partial x}\sin\delta = -\frac{\partial \hat{p}}{\partial y} + \hat{\theta}\cos\delta, \quad (11b)$$

$$\left(\frac{\partial}{\partial \tau} - \nabla^2\right)\hat{w} + G\bar{r}^*\bar{u}_v\frac{\partial \hat{w}}{\partial x}\sin\delta = -\frac{\partial \hat{p}}{\partial z}, \quad (11c)$$

$$\left(Pr\frac{\partial}{\partial \tau} - \nabla^2\right)\hat{\theta} + R\bar{a}^*\bar{u}_v\frac{\partial \hat{\theta}}{\partial x}\sin\delta + R\bar{a}^*\frac{d\bar{\theta}}{dy}\hat{v} = \frac{-(1-\omega)\tau_0^2\Gamma}{N}(4\hat{\theta} - \hat{j}), \quad (12)$$

$$[\nabla^2 - 3(1-\omega)\tau_0^2]\hat{j} = -12(1-\omega)\tau_0^2\hat{\theta}, \quad (13)$$

subject to the following boundary conditions:

$$\hat{u} = \hat{v} = \hat{w} = 0, \text{ at } y = 0, 1 \text{ (rigid walls)} \quad (14a)$$

$$\frac{\partial}{\partial y}\left(\hat{\theta} + \frac{\Gamma}{3N}\hat{j}\right) \mp H_i\hat{\theta} = 0, \text{ at } y = 0, 1, \quad (14b)$$

and the Marshak boundary conditions in terms of $\hat{j}$ given as [14]:

$$\frac{\partial \hat{j}}{\partial y} \mp \lambda_i(\hat{j} - 4\hat{\theta}) = 0, \text{ at } y = 0, 1. \quad (14c)$$

In the above definitions $R\bar{a}^*$ is the *external Rayleigh number* based on the difference between the environment temperature, $G\bar{r}^*$ is the *external Grashof number*, Pr is the *Prandtl number* and $\bar{u}_v(y)$ is the base flow velocity at the vertical position.

The formal solution of the linear stability equations (10–13) can be taken in the form:

$$\hat{F}(x,y,z,\tau) = F^*(y)\exp[i(a_1 x + a_2 z) + c\tau], \quad (15)$$

where, $\hat{F} = \hat{j}, \hat{p}, \hat{u}, \hat{v}, \hat{w}$ or $\hat{\theta}$, the quantity c is complex; a_1 and a_2 are the wave numbers in the x and z directions respectively. The solution (15) is introduced into the stability equations (10–14) and the variables p^*, u^* and w^* are eliminated among these resulting expressions. We obtain the following perturbation quations:

$$[c - (D^2 - a^2)](D^2 - a^2)v^* + ia_1 G\bar{r}^*\sin\delta[\bar{u}_v(D^2 - a^2) - D^2\bar{u}_v]v^* = -a^2\theta^*\cos\delta - ia_1 D\theta^*\sin\delta \quad (16)$$

$$[cPr-(D^2-a^2)]\theta^*+ia_1R\bar{a}\theta^*\sin\delta$$
$$+R\bar{a}D\bar{\theta}v^*=-\frac{(1-\omega)\tau_0^2\Gamma}{N}(4\theta^*-j^*) \quad (17)$$

$$[D^2-a^2-3(1-\omega)\tau_0^2]j^*=-12(1-\omega)\tau_0^2\theta^*. \quad (18)$$

Subject to the boundary conditions:

$$v^*=DV^*=D\left(\theta^*+\frac{\Gamma}{3N}j^*\right)\mp H_i\theta^*$$
$$=Dj^*\mp\lambda_i(j^*-4\theta^*)=0, \text{ at } y=0,1, \quad (19)$$

where

$$a^2=a_1^2+a_2^2,\ D=\frac{d}{dy}.$$

For the horizontal position, when the upper surface is free while the lower one is rigid, the boundary condition for opaque surface becomes unchanged but the velocity boundary condition at the upper surface takes the form:

$$V^*=D^2V^*=0, \text{ at } y=1 \text{ (free surface)}. \quad (20)$$

The onset of instability for the above system can either occur as stationary convective cells or in the form of travelling waves. It has been verified experimentally in references [15, 16], for CO_2 and water, that the onset of instability occurs as stationary cells. Furthermore, since the majority of fluid flow problems with pronounced effects of radiation are associated with gaseous media, (i.e., $Pr<1$), the instability in such a media is expected to set in as stationary rolls (i.e., $c=0$). These disturbances are dominated by two-dimensional waves and occur as either longitudinal or transverse rolls. For the case of a horizontal slender slot, the fluid being stagnant prior to the onset of instability, the two and three-dimensional analysis of the problem lead to the same result. It is experimentally verified that instability of the fluid results in a three-dimensional convective patterns called the Bénard hexagonal cells.

Longitudinal rolls ($a_1=0$). The governing equations are obtained by setting $c=a_1=0$ in equations (16–18). Then if θ^* is eliminated from the resulting expressions, we obtain:

$$(D^2-a_2^2)^2v^+(y)=a_2^2R\bar{a}\cos\delta(D^2-a_2^2-\kappa^2)j^+(y) \quad (21)$$

$$(D^2-a_2^2)(D^2-a_2^2-s^2)j^+(y)=D\bar{\theta}v^+(y), \quad (22)$$

where we defined

$$v^+(y)=-12(1-\omega)\tau_0^2R\bar{a}v^*(y),\ j^+=j^*$$
$$\kappa^2=3(1-\omega)\tau_0^2,\ s^2=3(1-\omega)\tau_0^2\left[1+\frac{4\Gamma}{3N}\right].$$

The boundary conditions for $v^+(y)$ and $j^+(y)$ for both convective rigid walls become:

$$v^+=DV^+=\xi_iDj^+\mp(D^2-a_2^2)j^+=0, \text{ at } y=0,1 \quad (23a)$$

$$D[D-a_2^2-s^2]j^+\mp H_i[D^2-a_2^2-\kappa^2]j^+=0, \text{ at } y=0,1,$$

for the case of free upper surface, the velocity boundary conditions at $y=1$ take the form

$$V^+=D^2V^+=0, \quad \text{at} \quad y=1. \quad (23b)$$

Transverse rolls ($a_2=0$). If the variable $v^*(y)$ appearing in equations (16–19) is replaced by the stream function $\psi^*(y)$ ($V^*=-ia_1\psi^*$), and c is set equal to zero, one obtains

$$(D^2-a_1^2)^2\psi^*(y)-ia_1Gr^*\sin\delta[\bar{u}_v(D^2-a_1^2)\psi^*$$
$$-D^2\bar{u}_v\psi^*]=[ia_1\theta^*\cos\delta-D\theta^*\sin\delta] \quad (24)$$

$$(D^2-a_1^2)\theta^*(y)-ia_1R\bar{a}[\bar{u}_v\theta^*\sin\delta$$
$$-D\bar{\theta}\psi^*]=\frac{(1-\omega)\tau_0^2\Gamma}{N}(4\theta^*-j^*) \quad (25)$$

$$[D^2-a_1^2-3(1-\omega)\tau_0^2]j^*(y)=-12(1-\omega)\tau_0^2\theta^*, \quad (26)$$

with the following boundary conditions for rigid walls:

$$\psi^*=D\psi^*=D\left(\theta^*+\frac{3\Gamma}{N}j^*\right)$$
$$\mp H_i\theta^*=Dj^*\mp\lambda_i(j^*-4\theta^*)=0,$$
$$\text{at } y=0,1. \quad (27)$$

Solutions of eigenvalue problems

In the present analysis, the equations governing the longitudinal and transverse rolls are solved by the "*Chardrasekhar Method*", because the convergence is fast for moderate Prandtl numbers [7, 8, 17].

(a) *Longitudinal rolls.* To solve the equations (21–23) governing the longitudinal rolls, an approximate solution is chosen for $V^+(y)$ as a series of orthogonal functions:

$$V^+(y)=\sum_{m=1}^{M}A_m\Phi_m(y), \quad (28a)$$

where the functions Φ_m are constructed from the solution of the following auxiliary problem:

$$\frac{d^4\Phi_m}{dy^4}=\alpha_m^4\Phi_m, \text{ in } 0<y<1, \quad (28b)$$

$$\Phi_m=D\Phi_m=0, \ y=0,1 \text{ (rigid walls)}, \quad (28c)$$

or

$$\Phi_m=D\Phi_m=0, \ y=0 \text{ (rigid wall)},$$
$$\Phi_m=D^2\Phi_m=0, \ y=1 \text{ (free surface)}. \quad (28d)$$

The functions $\Phi_m(y)$ satisfying the boundary conditions (28c) and (28d) are taken as:

$$\Phi_m(y)=\frac{\cosh\alpha_my-\cos\alpha_my}{\cosh\alpha_m-\cos\alpha_m}$$
$$-\frac{\sinh\alpha_my-\sin\alpha_my}{\sinh\alpha_m-\sin\alpha_m}, \quad (29)$$

where α_m's are the positive roots of:

$$\cosh\alpha\cos\alpha = 1 \text{ (both walls rigid)} \quad (30a)$$

$$\coth\alpha - \cot\alpha = 0 \text{ (upper surface free).} \quad (30b)$$

The orthogonality condition is given as

$$\int_0^1 \Phi_m \Phi_n \mathrm{d}y = \delta_{nm} N_m, \quad (31)$$

where δ_{nm} is the Kronecker delta and,

$$N_m = [\tanh\alpha_m \sinh\alpha_m]^{-2} \text{ (both walls rigid),}$$

or

$$N_m = \frac{2\tanh^2\alpha_m \sinh\alpha_m \sin\alpha_m (\cosh\alpha_m \cos\alpha_m - 1)}{(\sinh\alpha_m - \sin\alpha_m)^4}.$$

(upper surface free)

When the solution of $V^+(y)$ is introduced into equation (22) together with the expansion

$$j^+(y) = \sum_{m=1}^{M} A_m j_m(y), \quad (32a)$$

one finds

$$(\mathrm{D}^2 - a_2^2)(\mathrm{D}^2 - a_2^2 - s^2) j_m(y) = \mathrm{D}\bar{\theta}(y)\Phi_m(y), \quad (32b)$$

where $\mathrm{D}\bar{\theta}$ is obtainable from equation (8a) by differentiation. Equation (32b) is solved analytically for $j_m(y)$. Now introducing the solutions for $V^+(y)$ and $j^+(y)$ into equation (21) and utilizing the orthogonality condition (31), one obtains the following secular determinant for the evaluation of the eigenvalue, Ra^*,

$$\|B_{mn} - a_2^2 (Ra^* \cdot \cos\delta) B^*_{mn}\| = 0, \quad \text{for } n = 1, 2, 3, \ldots, M, \quad (33)$$

where

$$B_{mn} = \int_0^1 (\mathrm{D}^2 - a_2^2)^2 \Phi_m(y)\Phi_n(y)\mathrm{d}y \quad (34a)$$

$$B^*_{mn} = \int_0^1 (\mathrm{D}^2 - a_2^2 - \kappa^2) j_m(y) \Phi_n(y)\mathrm{d}y. \quad (34b)$$

The minimum (i.e., critical) value of Ra^* is established from the solution of equations (33) as a function of the wave number, a_2, for each given set of system parameters (H_1, H_2, J, N, τ_0, ω, ε_1, ε_2 and η).

(b) *Transverse rolls.* The differential equations governing the transverse rolls (24–27) are complex. As a result, the solution of this system should be complex. The work presented in reference [14], with radiation being neglected indicated that the critical Rayleigh number is indeed insensitive to variations of the Biot numbers H_1 and H_2. The radiation being considered here in this analysis, it is expected that the effect of the Biot numbers should be quite negligible. Therefore, the effect of H_1 and H_2 is omitted from the analysis of the transverse rolls by letting $H_1 = H_2 \to \infty$ (i.e., fixed wall temperatures). To solve the system of equations (24–27) for $H_1 = H_2 \to \infty$, by the Chandrasekhar method, complex solutions for ψ^* and θ^* are constructed as

$$\psi^*(y) = \psi_1^* + i\psi_2^*, \quad \theta^*(y) = \theta_1^* + i\theta_2^*. \quad (35a)$$

The solution (35a) being complex, another set of solution exists as

$$\psi^*(y) = \psi_1^* + i\psi_2^*, \quad \theta^*(y) = \theta_2^* + i\theta_1^*. \quad (35b)$$

Although there are two other possibilities, they are the same as either (35a) or (35b). The solutions are taken as

$$\psi_1 = \sum_{m=1}^{M} A_m \phi_{2m-1}(y), \quad \psi_2^* = \sum_{m=1}^{M} B_m \phi_{2m}(y)$$
$$\theta_1^* = \sum_{m=1}^{M} C_m \theta_{2m}(y), \quad \theta_2^* = \sum_{m=1}^{M} D_m \theta_{2m-1}(y), \quad (36)$$

where, the orthogonal functions $\phi_m(y)$ are developed previously and given by equation (29) with the auxiliary eigenvalues α_m's from (30a) and the orthogonality condition (31). It is to be noted that for the case of two rigid walls only, the constructed functions ψ_1^* and ψ_2^* given by equations (36) are similar to those reported in reference [18], such that ψ_1^* is even and ψ_2^* is odd. The orthogonal functions $\theta_m(y)$ which satisfy the boundary conditions (27) for $H_i \to \infty$ are taken as:

$$\theta_m(y) = \sin\beta_m y, \quad \beta_m = m\pi. \quad (37)$$

The known solutions for $\theta^*(y)$ are introduced into equation (26), the resulting expression for j^* is integrated subjected to the boundary conditions (27) for j^* to obtain

$$j^* = j_1^* + ij_2^* \quad \text{or} \quad j^* = j_2^* + ij_1^*, \quad (38a)$$

with

$$j_1^*(y) = 12(1-\omega)\tau_0^2 \sum_{m=1}^{M} C_m j_{m_1}(y)$$
$$j_2^*(y) = 12(1-\omega)\tau_0^2 \sum_{m=1}^{M} \mathrm{D}_m j_{m_2}(y), \quad (38b)$$

where $j_{m_i}(y)$ is obtainable from the solution of the following system:

$$(\mathrm{D}^2 - a^2 - 3(1-\omega)\tau_0^2) j_{m_i} = -\theta_{m_i}(y), \quad i = 1, 2$$
$$\mathrm{D}j_{m_i} \mp \lambda_i j_{m_i} = 0, \text{ at } y = 0, 1. \quad (39)$$

Having determined the complex solutions for $j^*(y)$ as given above the problem defined by equations (24–26) now reduces to two equations (24) and (25) only in terms of the complex functions ψ^* and θ^*. Then the constructed solutions (35) for ψ^* and θ^* together with the solution for j^* are introduced into these equations, and the real and imaginary parts of each equation are separated. By utilizing the orthogonality condition for each of the resulting four equations, the end result leads to the following characteristic equation whose zeros establish the eigenvalues, Ra^*,

$$\|y_{nm}\| = 0, \text{ for } n = 1, 2, 3, \ldots,$$

where the elements y_{nm} are real matrices of order $4N \times 4N$ arising from the orthogonalization of equations (24) and (25), M being the number of approximations considered in equations (36).

RESULTS AND CONCLUSIONS

To study the effects of each system parameter on the conditions marking the onset of instability, two different Rayleigh numbers are defined. One of these is the critical internal Rayleigh number Ra_c which is based on the unknown difference between the initial wall temperatures $(\bar{T}_{w1} - \bar{T}_{w2})$ and the other is the critical external Rayleigh number $R\bar{a}_c^*$ which is defined on the basis of the difference between the external environment temperatures $(T_{\infty 1} - T_{\infty 2})$. The relation between these two Rayleigh numbers is given as

$$Ra_c = \left[\frac{\bar{T}_{w1} - \bar{T}_{w2}}{T_{\infty 1} - T_{\infty 2}}\right] \cdot R\bar{a}_c^*, \tag{41a}$$

where the temperature ratio is obtained from equation (8a) as

$$\frac{\bar{T}_{w1} - \bar{T}_{w2}}{T_{\infty 1} - T_{\infty 2}} = -[A_1(e^s - 1) + A_2(1 - e^{-s}) + A_3]. \tag{41b}$$

The external Rayleigh number $R\bar{a}^*$ is a more convenient criterion to use under convective boundary conditions because the temperature difference involved is known; but in this study the internal Rayleigh number is used in order to facilitate the comparison of the results with that for the case of fixed wall temperatures.

In the present study the calculations are performed for a fluid having a Prandtl number 0.72, because, the effects of radiation are more pronounced with a gaseous media. In discussing below the results for the effects of various system parameters on stability, the cases of "both rigid walls" and "lower surface rigid and upper surface free" are considered separately.

Both walls rigid

In Fig. 2 the critical Rayleigh number, Ra_c, computed for Bénard cells is plotted as a function of the optical thickness τ_0 for the values of conduction-to-radiation parameter $N = 1$ and 0.1, ($\varepsilon_1 = \varepsilon_2 = 1$, $\omega = 0$, $\eta = 1$ and $\delta = 0$) and for several different values of the identical Biot numbers H_1 and H_2. As shown in this figure, for the non-radiating case (i.e., $\tau_0 = 0$), the critical internal Rayleigh number Ra_c decreases with decreasing Biot numbers H_1 and H_2 as discussed in [19–21]. When radiation is present, the stability is improved due to the smoothing of the medium temperature resulting from the drain of energy from the hotter to the colder region by radiation in addition to that by conduction. The effect of the Biot numbers on stability is less pronounced with increased radiation resulting from either a decrease in N or an increase in τ_0. The reason for this is that when radiation increases the conduction effects become less important.

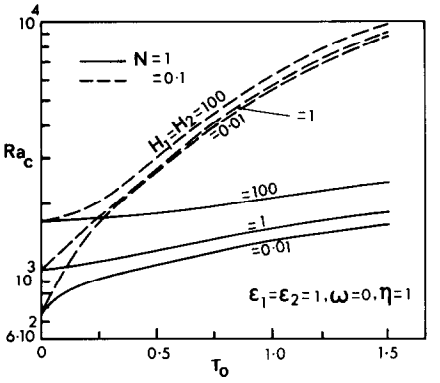

FIG. 2. Variation of critical internal Rayleigh number Ra_c for a gray gas with H_1 and H_2 and the radiation parameters N and τ_0.

To illustrate the effects of radiation on the stability of the fluid at any inclination, we present in Figs 3(a) and (b) the critical Grashof number Gr_c for the case of fixed wall temperatures (i.e., $Gr_c = G\bar{r}_c^*$) plotted as a function of the positive inclination angle (i.e., $0 \leqslant \delta \leqslant 90$) and various values of the optical thickness τ_0 ranging from 0 to ∞, for $N = 1$, 0.1 and $Pr = 0.72$. Figure 3(a) is prepared for $N = 1$. In this figure, the critical Grashof number, Gr_c, for the longitudinal rolls at any angle δ, is shown by the dotted lines. When longitudinal rolls are dominant, the critical Grashof number at any inclination is related to the critical Grashof number at the horizontal position by $Gr_c = Gr_{cH}/\cos\delta$, as is apparent from equation (21). Whereas, when transverse rolls are dominant, the inclination angles "δ" have a very little effect on the

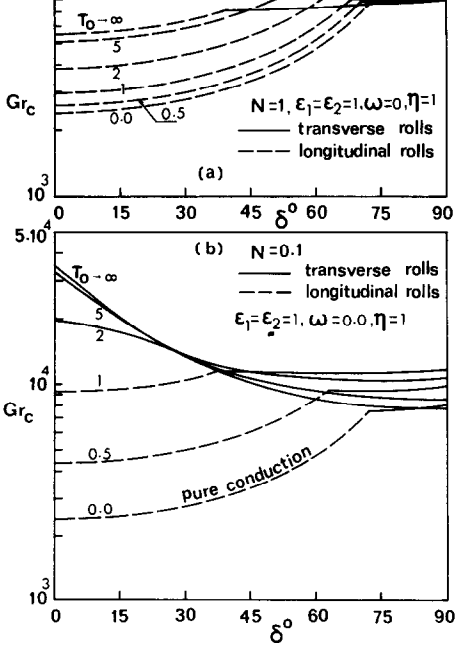

FIG. 3. Variation of the critical Grashof number Gr_c versus the positive inclination angle δ and the optical thickness τ_0 of a gray gas for the cases: (a) $N = 1$ and (b) $N = 0.1$.

critical Grashof number. The reason for this can be explained as follows: Transverse rolls are controlled by the combined effects of dynamic forces or inertia forces developed from the base flow velocity and the perturbed buoyancy forces in both the x and z directions. For Prandtl number Pr of order of unity and with radiation being neglected, the instability is almost initiated due to the effect of the inertia forces because buoyancy forces have a very little influence when transverse rolls are dominant [14]. This conclusion is opposite to that for lingitudinal rolls, in which the instability sets in due to the top-heavy arrangement created by heating the fluid from the underside. In this case, the longitudinal rolls are only controlled by the component of the buoyancy force in the y-direction as shown in equation (21), which is solely dependent on the temperature boundary conditions represented by the Biot numbers. When radiation exists, its influence on the magnitude of the velocity is small compared to that on the temperature distribution. As a result, the effect of radiation, when transverse rolls are dominant, is less pronounced than that when longitudinal rolls have a priority of occurrence over transverse rolls.

Figure 3(a) illustrates the cross-over from the longitudinal rolls to the transverse rolls defined by the transition angle "δ_t" as a function of the optical thickness τ_0, for $N = 1$ and ($\omega = 0$, $\eta = 1$, $\varepsilon_1 = \varepsilon_2 = 1$). Clearly, increasing the optical thickness τ_0 from to ∞ decreases the crossover angle δ_t from a value of 72° for the case of pure conduction to 39° for $\tau_0 \to \infty$. For moderate radiation (i.e., $N = 1$, $\tau_0 = 1$), this transaction angle is about $\delta_t = 69°$. Figure 3(b) is plotted for $N = 0.1$ while keeping the other parameters the same as those for Fig. 3(a). This figure implies that as radiation becomes stronger, the transition angle shifts toward the horizontal at a much faster rate such that for $\tau_0 > 1$ the transverse rolls are dominant for all inclinations except at the horizontal, in which both types of the disturbances are identical and replaced by the Bérnard Cells. Therefore, for $\tau_0 > 1$, the maximum stabilizing effects of the radiation occur at the horizontal position if the fluid is heated from below. The reason for this is attributed to the fact that transverse rolls are created by the combined effects of the inertia forces and the perturbed buoyancy forces in the x and y-directions. At the horizontal position, both the inertia forces and the x-component of buoyancy force vanish as shown in equation (24) and stability is controlled by the y-component of the disturbed buoyancy force only which is solely dependent on the radiation transfer. As the angle δ increases, inertia forces build up very fast and enhance the onset of instability since their dependence on radiation are much less than that of the buoyancy forces. For angles near the vertical, the critical Grashof number approaches the limiting value for the pure conduction as $\tau_0 \to \infty$.

Figure 4(a) shows the critical Grashof number for three positive values of inclination angles $\delta = 0$, 30 and 60° and for $N = 1$, 0.1, while Fig. 4(b) shows it

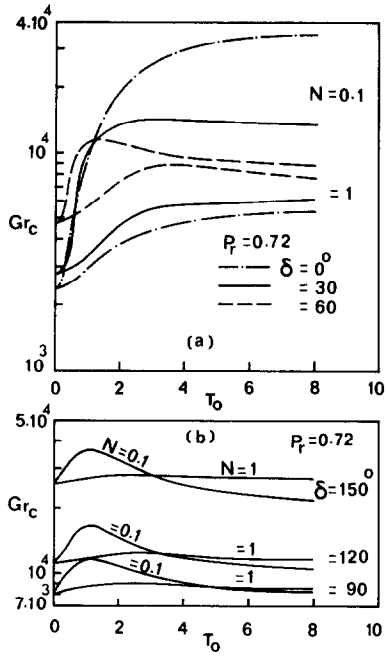

FIG. 4. Variation of the critical Grashof number Gr_c versus the radiation parameters N and τ_0 of gray gases for the cases: (a) $\delta = 0$, 30 and 60° and (b) $\delta = 90$, 120 and 150.

for angles $\delta = 90$, 120 and 150°. When the angle δ is greater than 90°, the physical situation corresponds to an inclined slot heated from the above sidewall. For $N = 1$, the critical Grashof number, Gr_c, increases with increasing the optical thickness τ_0; but, for angles $\delta \geqslant 60°$, the Grashof number reaches a maximum value and then starts to decrease very slowly. For $N = 0.1$, the critical Grashof number increases monotonically for the Bénard Problem (i.e., $\delta = 0$) whereas it assumes a maximum for the other inclinations. For the conduction regime considered here, for angles $90° \leqslant \delta < 180°$, transverse rolls are always dominant for all values of the optical thickness τ_0 including the case $\tau_0 = 0$, corresponding to the pure conduction problem.

The effects of single scattering albedo ω on the critical Rayleigh number, Ra_c, for $\varepsilon_1 = \varepsilon_2 = 1$, $\eta = 1$, $H_1 = H_2 = 100$, and $\delta = 0$ are shown in Fig. 5. As expected, the increased value of ω, which corresponds to increased scattering, decreases stability because the interaction of radiation with conduction and convection is decreased with increasing value of ω.

Figure 6 illustrates the effects of the wall emissivities ε_1 and ε_2 on the critical Rayleigh number Ra_c for $H_1 = H_2 \to \infty$, $\omega = 0$, $\eta = 1$, and $\delta = 0$. The stability is improved with reducing the wall emissivities specially for strong radiation. The reason for this, is attributed to the fact that the base flow temperature distribution becomes flatter with mirror boundaries (i.e., $\varepsilon = 0$), than with black surfaces (i.e., $\varepsilon = 1$).

Finally, Fig. 7 is prepared to illustrate the first order effects of nongrayness factor η on the critical

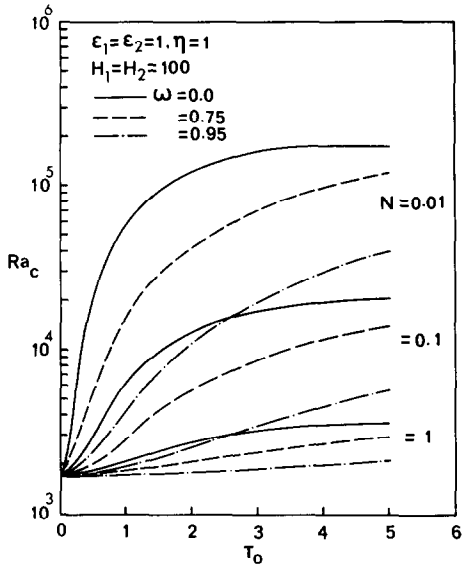

FIG. 5. Effect of single scattering albedo ω on the critical internal Rayleigh number Ra_c at $\delta = 0°$; for various values of N and τ_0 for a gray gas.

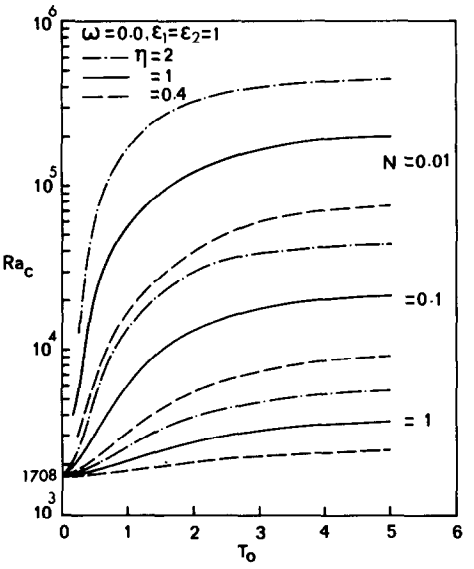

FIG. 7. Effect of nongrayness factor η on the critical internal Rayleigh number Ra_c at $\delta = 0°$, for different values of N and τ_0.

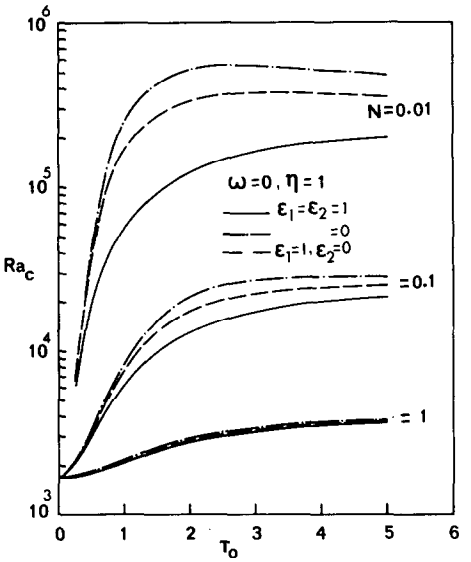

FIG. 6. Effects of the wall emissivities ε_1 and ε_2 on the critical internal Rayleigh number Ra_c versus radiation parameters N and τ_0 at the horizontal position for a gray gas.

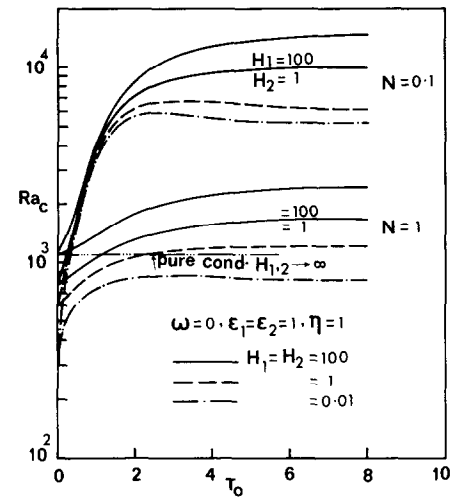

FIG. 8. Effects of Biot numbers H_1 and H_2 and the radiation parameters N and τ_0 on Ra_c for the case of lower surface rigid and upper one free.

Rayleigh number for $\varepsilon_1 = \varepsilon_2 = 1$, $\omega = 0$, $H_1 = H_2 \to \infty$, and $\delta = 0$. The range of η chosen from 0.4 to 2 is considered reasonable for gases [22]. The assumption of constant η used in this analysis is applicable for either small temperature difference or small pressure variations. Stability is significantly improved with increased value of η especially for smaller values of N. The reason for the stabilizing effect of increased value of η can be explained as follows: This factor, by definition, is the ratio of the Planck mean to Rosseland mean coefficients. The Planck mean being associated with the emission of radiation, and the Rosseland mean with the absorption of radiation by the medium, the increased value of η (i.e., $\eta > 1$) tends to drain more energy from the hotter region to the colder one, which, in turn, makes the temperature distribution more smooth compared with the case of small η, and as a result the onset of cellular convection is delayed. A more realistic model for the representation of the nongrayness can be used, but the complication arising from the increased algebraic involvement in the problem, makes it difficult to get a solution.

Figure 7 shows the first order effects of nongrayness on the instability phenomena for the horizontal position characterized by the Bérnard Cells. Here in Table 1, we illustrate the effect of the nongrayness factor η on the critiçal Grashof number, Gr_c, for ω

Table 1. An illustration of the variation of Gr_c by the nongrayness factor η ($\omega = 0$, $\tau_0 = 2$, $\delta = 90°$, $H_1 = H_2 \to \infty$, $Pr = 0.72$)

		Gr_c for $N = 1$			Gr_c for $N = 0.1$		
ε_1	ε_1	$\eta = 0.4$	$\eta = 1$	$\eta = 4$	$\eta = 0.4$	$\eta = 1$	$\eta = 4$
1	1	8320	8960	12251	9061	10740	19022
1	0	8590	9380	13384	11860	15600	27920
0	0	8814	9820	14460	14431	20600	36783

$= 0$, $\tau_0 = 2$, $\delta = 90°$, $Pr = 0.72$ and $H_1 = H_2 \to \infty$. The nongrayness associated with transverse rolls is the most important parameter which has a strong effect on the initiation of the cellular convection; but this effect is less than that for the Bérnard Cells for the reasons stated previously.

Lower surface rigid and upper one free

For the horizontal case, when the upper surface is exposed directly to the surrounding, the shear stress associated with the vertical disturbed velocity $v^*(y)$ vanishes at this surface, and the onset of instability for this situation is expected to occur earlier than the case of "both walls rigid". Figure 8 shows the effects of the Biot numbers H_1 for the lower wall and H_2 for the upper surface on the critical internal Rayleigh number for $\delta = 0$, $\omega = 0$, $\varepsilon_1 = \varepsilon_2 = 1$ and $\eta = 1$. This figure has a similar behavior as Fig. 2, except that the variations of Ra_c with H_1 and H_2 are much more pronounced in this case than with two rigid walls. Although this figure is prepared for $\varepsilon_1 = \varepsilon_2 = 1$, other combinations of wall emissivity are also examined. The combinations other than $\varepsilon_1 = \varepsilon_2 = 1$ gave slightly improved stability criteria.

An examination of the convergence of the results computed from the analysis of the longitudinal rolls revealed that the largest difference between the second and first approximation about 1.3%. The computational results for transverse rolls are carried out by using the scientific subroutine "LADATF" for determinants of orders 8×8, 12×12 and 16×16. The difference between the results of 16×16 and 12×12 determinants is less than 0.30 percent. Also, the first solution defined by equation (35a) gives a critical Rayleigh number which is always less than that obtained from the second solution (35b) for all combinations of the input system parameters.

Acknowledgement—This work was performed in part through the National Science Foundation Grant ENG 77-12949.

REFERENCES

1. R. M. Goody, The influence of radiative transfer on cellular convection, *J. Fluid Mech.* **1,** 424–435 (1966).
2. S. H. Davis, On the principle of exchange of stabilities, *Proc. R. Soc.* **A310,** 341–358 (1969).
3. C. Christophorides and S. H. Davis, Thermal instability with radiative transfer, *Phys. Fluids* **13,** 222–226 (1970).
4. E. A. Speigel, The convective instability of a radiating fluid layer. *Astrophys. J.* **132,** 715–728 (1960).
5. J. Gille and R. Goody, Convection in a radiating gas, *J. Fluid Mech.* **20,** 47–79 (1964).
6. V. S. Arpaci and D. Gözüm, Thermal stability of radiating fluids: The Benard problem, *Phys. Fluids* **16,** 581–589 (1973).
7. V. S. Arpaci and Y. Bayazitoğlu, Thermal stability of radiating fluids, *Phys. Fluids* **16,** 589–593 (1973).
8. M. N. Özişik and M. A. Hassab, Stability of gas in the gap of inclined flat plate solar Collectors—effect of convective boundary conditions and radiation, in *Alternative Energy Sources*, edited by T. N. Veziroğlu, Vol. 1, pp. 199–218. Hemisphere, New York (1979).
9. R. G. Brooks and S. D. Probert, Heat transfer between parallel walls: An interferometric investigation, *J. Mech. Engng Sci.* **14,** 107–127 (1972).
10. K. R. Randall, M. M. El-Wakil and J. W. Mitchell, Natural convection characteristics of flat plate collectors, *U.S. Energy Research and Development Administration Contract E*(11-1)—2971, April (1977).
11. S. C. Traugott, Radiative heat-flux potential for a nongray gas, *AIAA J.* **4,** 541–542 (1966).
12. A. C. Cogley, W. C. Vincenti and S. E. Gilles, Differential approximation for radiative transfer in a nongray gas near equilibrium, *AIAA J.* **6,** 551–553 (1968).
13. S. E. Gilles, A. C. Cogley and W. G. Vincenti, A substitute kernal approximation for radiative transfer in a nongray gas near equilibrium, with application to radiative acoustics, *Int. J. Heat Mass Transfer* **12,** 445–458 (1969).
14. M. A. Hassab, Thermal stability of natural convection in slots and flow down an inclined heated plane, Ph.D. Thesis, North Carolina State University at Raleigh, Dept. of Mechanics and Aerospace Engineering (1978).
15. C. Mordchhelles-Regnier and C. Kaplan, Visualization of natural convection of a plane wall and in a vertical gap by differential interferometry. Transitional turbulent regime, *Proc. Heat Trans. Fluid Mech. Inst.* 94–111 (1963).
16. J. Hart, Stability of the flow in a differentially heated inclined box, *J. Fluid Mech.* **47,** 547–576 (1971).
17. S. Chandrasekhar, *Hydrodynamic and Hydromagnetic Stability*, pp. 23, Oxford University Press (1961).
18. D. L. Harris and W. H. Reid, On orthogonal functions which satisfy four boundary conditions, *Astrophys. J. Suppl.* Ser. 3, 429–447 (1958).
19. E. M. Sparrow, R. J. Goldstein and V. K. Jonsson, Thermal instability in a horizontal fluid layer; Effect of boundary conditions and non-linear temperature profile, *J. Fluid Mech.* **18,** 513–528 (1964).
20. E. M. Sparrow, L. Lee and N. Shamsundar, Convective instability in a melt layer heat from below, *J. Heat Transfer* **98C,** 88–94 (1976).
21. M. A. Hassab and M. N. Özişik, Stability of a layer of fluid subjected to convective boundary conditions, *Int. J. Heat Mass Transfer* **21,** 1264–1266 (1978).
22. D. H. Sampson, *Radiative Contributions to Energy and Momentum in a Gas*. John Wiley, New York (1965).

EFFET DU RAYONNEMENT ET DES CONDITIONS AUX LIMITES DE CONVECTION SUR LA STABILITE D'UN FLUIDE DANS UNE FENTE INCLINEE

Résumé—Pour une inclinaison variant entre 0° et 180°, on étudie la stabilité neutre d'un fluide visqueux absorbant émissif, diffusant et non-gris contenu dans une cavité allongée et soumise à des conditions aux limites de convection. L'approximation modifiée $P-1$ (approximation d'Eddington) est utilisée. On détermine à la fois pour les rouleaux tourbillonnaires longitudinaux et transverses, les effets des nombres de Biot H_1 et H_2 sur les surfaces, du paramètre conduction-rayonnement N, de l'épaisseur optique τ_0, de l'albedo de diffusion ω, des émissivités ε_1 et ε_2, du facteur η et de l'angle d'inclinaison δ, sur les conditions de stabilité dans les gaz. Les résultats montrent que le rayonnement, outre son effet stabilisant, déplace nettement l'angle correspondant au basculement des tourbillons.

DER EINFLUSS VON STRAHLUNGS- UND KONVEKTIONS-RANDBEDINGUNGEN AUF DIE STABILITÄT EINES FLUIDES IN EINEM GENEIGTEN SCHMALEN SPALT

Zusammenfassung—Es wird die neutrale Stabilität eines absorbierenden, emittierenden, streuenden, nicht-grauen viskosen Fluides untersucht, welches sich innerhalb eines geneigten Spalts befindet und konvektiven Randbedingungen ausgesetzt ist. Die Neigung beträgt 0° bis 180°. Zur Lösung des Strahlungsproblems wird die modifizierte P-1 Approximation (Eddington Approximation) eingesetzt. Die Einflüsse der Biot-Zahlen H_1 und H_2 für die untere und obere Grenzfläche, des Verhältnisses von Leitung zu Strahlung N, der optischen Dicke τ_0, des Reflexionswinkels ω der einfachen Streuung, der Emissivitäten ε_1 und ξ_2 der Wand, des Faktors η für die Abweichung vom grauen Strahler und des Neigungswinkels δ auf das Einsetzen der Stabilität in Gasen werden für longitudinale und transfersale Wirbelrollen bestimmt. Die Ergebnisse zeigen, daß die Strahlung neben ihrer stabilisierenden Wirkung vor allem den Übergangswinkel für den Umschlag von transversalen zu longitudinalen Wirbelrollen in Richtung der Horizontalen verschiebt.

ВЛИЯНИЕ ЛУЧИСТЫХ И КОНВЕКТИВНЫХ ГРАНИЧНЫХ УСЛОВИЙ НА УСТОЙЧИВОСТЬ ЖИДКОСТИ В НАКЛОНЁННОМ НЕБОЛЬШОМ ЩЕЛЕВОМ КАНАЛЕ

Аннотация — Исследуется нейтральная устойчивость поглощающей, отражающей и рассеивающей несерой вязкой жидкости в узком зазоре наклонного канала в диапазоне углов от 0 до 180° при граничных условиях третьего рода. Процесс излучения учитывался с помощью модифицированного P-I приближения (приближение Эддингтона). Определялось влияние чисел Био, H_1 и H_2, для нижней и верхней поверхностей, лучисто-кондуктивного параметра N, оптической толщины τ_0, единичного коэффициента диффузно-рассеивающего отражения ω, коэффициентов излучения стенок ε_1 и ε_2, коэффициента несерого излучения η и угла наклона δ на возникновение устойчивости в газах как для продольных, так и поперечных вихревых валов. Результаты свидетельствуют о том, что помимо стабилизирующего воздействия излучение существенно смещает к горизонтали угол, при котором происходит переход поперечных валов в продольные.